Spiroalkanedithiol-Based SAMs Reveal Unique Insight into the Wettabilities and Frictional Properties of Organic Thin Films

Young-Seok Shon, Seunghwan Lee, Ramon Colorado, Jr., Scott S. Perry,* and T. Randall Lee*

Contribution from the Department of Chemistry, University of Houston, Houston, Texas 77204-5641

Received February 3, 2000

Abstract: Self-assembled monolayers (SAMs) were prepared by the adsorption of a series of 2,2-dialkylpropane-1,3-dithiols (**1**−**5**) and 2-pentadecylpropane-1,3-dithiol (**6**) onto the surface of gold. These SAMs were characterized by ellipsometry, contact angle goniometry, X-ray photoelectron spectroscopy (XPS), polarization modulation infrared reflection absorption spectroscopy (PM-IRRAS), and atomic force microscopy (AFM). The studies demonstrate that a systematic variation in the structure of $R'RC(CH_2SH)_2$ from symmetrical (**1**; $R' = R$) to progressively more unsymmetrical (**2**−**6**; $R' \neq R$) can be used to provide control over the conformational order and interchain packing of the hydrocarbon tail group assembly. The tail group conformation and packing were found to influence profoundly both the wettability and the tribological properties of the SAMs. Assemblies of well-ordered, well-packed hydrocarbon tail groups yielded interfaces that exhibited low wettabilities and low frictional responses when compared to assemblies of disordered, loosely packed hydrocarbon tail groups. The trends in wettability and friction were rationalized by considering the magnitude of the van der Waals interactions between the hydrocarbon film and the contacting probe liquid and AFM tip, respectively.

Introduction

Controlling the nanoscale structure and properties of interfaces remains a challenging enterprise.[1] The ability to dictate the wettabilities and frictional properties of solid surfaces offers technological advances in materials applications ranging from paints to lubricants.[2−5] Organic thin films, such as self-assembled monolayers (SAMs) generated by the adsorption of organic moieties onto solid surfaces, have been widely used to modify the interfacial properties of the underlying substrates.[6] In particular, the adsorption of long-chain alkanethiols onto the surfaces of metals provides a useful and versatile strategy for modifying the interfacial properties of metallic interfaces.[6−9] Moreover, the adsorption of mixtures of two or more distinct alkanethiols can be used to generate structurally complex interfaces containing a mixture of different chemical functionalities and/or chain lengths.[10−17] These latter systems, however, often suffer from the problem that the adsorbates distribute themselves inhomogeneously across the surface,[10−12] forming readily detectable domains or "islands" of individual adsorbates in many cases.[13,15,16,18] The problem of islanding in mixed SAMs has hindered progress toward understanding the interfacial properties of multicomponent organic surfaces, such as those commonly encountered in polymeric and biological systems.

Recently, we reported a convenient strategy for preparing homogeneously mixed multicomponent SAMs via the adsorption of unsymmetrical 2,2-dialkylpropane-1,3-dithiols, which we call "spiroalkanedithiols", onto the surface of gold.[18] These studies revealed that mixed SAMs generated from this class of adsorbate exhibited homogeneous lateral chain distributions and distinct frictional properties when compared to SAMs generated from mixtures of normal alkanethiols having analogous chain lengths. Specifically, we found evidence of islanding and low friction for the SAMs derived from the mixtures of normal alkanethiols, but no islanding and higher friction for the SAMs derived from the unsymmetrical spiroalkanedithiols.

In the present work, we generate and characterize SAMs derived from the symmetrical 2,2-dipentadecylpropane-1,3-dithiol (**1** in Figure 1) and from a series of unsymmetrical derivatives of **1** in which one of the chain lengths is systematically varied (**2**−**6** in Figure 1). Due to their unique structure (two distinct tail groups connected via a single carbon atom),

(1) Swalen, J. D.; Allara, D. L.; Andrade, J. D.; Chandross, E. A.; Garoff, S.; Israelachvili, J.; McCarthy, T. J.; Murray, R.; Pease, R. F.; Rabolt, J. F.; Wynne, K. J.; Yu, H. *Langmuir* **1987**, *3*, 932.
(2) Laibinis, P. E.; Whitesides, G. M.; Allara, D. L.; Tao, Y.-T.; Parikh, A. N.; Nuzzo, R. G. *J. Am. Chem. Soc.* **1991**, *113*, 7152.
(3) Chaudhury, M. K.; Whitesides, G. M. *Science* **1992**, *255*, 1230.
(4) Bhushan, B.; Israelachvili, J. N.; Landman, U. *Nature* **1995**, *374*, 607.
(5) Hsu, S. M. *Langmuir* **1996**, *12*, 4482.
(6) Ulman, A. *Thin Films−Self-Assembled Monolayers of Thiols*; Academic: Boston, 1998.
(7) Bain, C. D.; Troughton, E. B.; Tao, Y.-T.; Evall, J.; Whitesides, G. M.; Nuzzo, R. G. *J. Am. Chem. Soc.* **1989**, *111*, 321.
(8) Nuzzo, R. G.; Dubois, L. H.; Allara, D. L. *J. Am. Chem. Soc.* **1990**, *112*, 558.
(9) Dubois, L. H.; Zegarski, B. R.; Nuzzo, R. G. *J. Am. Chem. Soc.* **1990**, *112*, 570.
(10) Bain, C. D.; Evall, J.; Whitesides, G. M. *J. Am. Chem. Soc.* **1989**, *111*, 7155.
(11) Bain, C. D.; Whitesides, G. M. *J. Am. Chem. Soc.* **1989**, *111*, 7164.
(12) Folkers, J. P.; Laibinis, P. E.; Whitesides, G. M. *Langmuir* **1992**, *8*, 1330.
(13) Folkers, J. P.; Laibinis, P. E.; Whitesides, G. M.; Deutch, J. *J. Phys. Chem.* **1994**, *98*, 563.
(14) Jin, Z. H.; Vezenov, D. V.; Lee, Y. W.; Zull, J. E.; Sukenik, C. N.; Savinell, R. F. *Langmuir* **1994**, *10*, 2662.
(15) Stranick, S. J.; Parikh, A. N.; Tao, Y.-T.; Allara, D. L.; Weiss, P. S. *J. Phys. Chem.* **1994**, *98*, 7636.
(16) Tamada, K.; Hara, M.; Sasabe, H.; Knoll, W. *Langmuir* **1997**, *13*, 1558.
(17) Imabayashi, S.; Gon, N.; Sasaki, T.; Hobara, D.; Kakiuchi, T. *Langmuir* **1998**, *14*, 2348.
(18) Shon, Y.-S.; Lee, S.; Perry, S. S.; Lee, T. R. *J. Am. Chem. Soc.* **2000**, *122*, 1278.

10.1021/ja000403z CCC: $19.00
Published on Web 07/19/2000

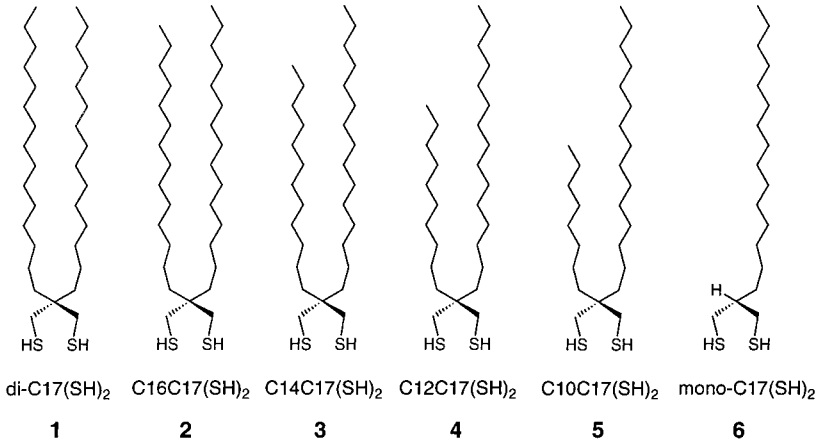

Figure 1. Structures of the spiroalkanedithiol adsorbates **1**−**6** used for generating SAMs on gold.

SAMs generated from **1**−**6** appear ideally suited for controlling the nanoscale topographic roughness and local order (i.e., crystalline packing) of the organic thin film interface. In addition, SAMs **1**−**6** offer the possibility of engineering metal surfaces in which the wettabilities and the frictional properties can be tailored with molecular-level precision.

The wetting of solid surfaces by liquids is largely influenced by the nature of the intermolecular forces that exist between these contacting media.[3,8,9] Several factors including (1) the chemical composition of the tail groups on the surface,[7−10] (2) the length of the alkyl chains,[11] and (3) phase separation (or islanding) in films derived from a mixture of adsorbates[12,13,17] can profoundly influence the magnitude of the interfacial forces. Since the preparation of SAMs from the chelating adsorbates **1**−**6** and related systems[19] necessarily precludes nanometer-scale islanding on the surface,[18] we wish to examine SAMs derived from these species to understand the relationship(s) between wettabilty and nanoscale roughness and order of the surface.[18]

In addition to studies of wettability, herein we explore the frictional properties of these films, which were measured using atomic force microscopy (AFM). Previous studies of friction by AFM have shown that the frictional properties of SAMs are sensitive to the packing density and crystallinity of the alkyl chains.[20−23] Consequently, the high degree of control over the local packing structure of the alkyl chains afforded by SAMs generated from chelating adsorbates **1**−**6**,[18] when combined with the nanoscale sensitivity of AFM, offers an unprecedented opportunity to explore the molecular-level factors that govern friction and lubrication in organic thin film systems.[22−26]

Experimental Section

Preparation of Adsorbates. Details of the synthesis of the 2,2-dipentadecylpropane-1,3-dithiol (**1**; di-C17(SH)$_2$) and 2-pentadecylpropane-1,3-dithiol (**6**; mono-C17(SH)$_2$) were provided in previous reports.[27,28] Compounds **2**−**5** were prepared similarly; complete analytical data for these new adsorbates are provided in the following four paragraphs.

2-Pentadecyl-2-tetradecylpropane-1,3-dithiol (2; C16C17(SH)$_2$). ^{1}H NMR (300 MHz, $CDCl_3$): δ 2.52 (d, J = 9.3 Hz, 4 H, SCH_2), 1.40−1.18 (m, 54 H), 1.08 (t, J = 9.3 Hz, 2 H, SH), 0.88 (t, J = 7.7 Hz, 6 H, CH_3). ^{13}C NMR (75 MHz, $CDCl_3$): δ 39.75, 33.64, 31.91, 30.42, 30.30, 29.65, 29.55, 29.48, 29.45, 29.38, 29.32, 22.64, 14.10. Anal. Calcd for $C_{32}H_{66}S_2$: C, 74.63, H, 12.92. Found: C, 74.76, H, 12.79.

2-Dodecadecyl-2-pentadecylpropane-1,3-dithiol (3; C14C17(SH)$_2$). ^{1}H NMR (300 MHz, $CDCl_3$): δ 2.52 (d, J = 9.3 Hz, 4 H, SCH_2), 1.37−1.19 (m, 50 H), 1.08 (t, J = 9.3 Hz, 2 H, SH), 0.88 (t, J = 7.7 Hz, 6 H, CH_3). ^{13}C NMR (75 MHz, $CDCl_3$): δ 39.76, 33.61, 31.91, 30.45, 30.25, 29.68, 29.53, 29.50, 29.45, 29.38, 29.30, 22.68, 14.12. Anal. Calcd for $C_{30}H_{62}S_2$: C, 74.00, H, 12.83. Found: C, 74.40 H, 12.64.

2-Decyl-2-pentadecylpropane-1,3-dithiol (4; C12C17(SH)$_2$). ^{1}H NMR (300 MHz, $CDCl_3$): δ 2.52 (d, J = 9.3 Hz, 4 H, SCH_2), 1.39−1.20 (m, 46 H), 1.08 (t, J = 9.3 Hz, 2 H, SH), 0.88 (t, J = 7.7 Hz, 6 H, CH_3). ^{13}C NMR (75 MHz, $CDCl_3$): δ 39.75, 33.63, 31.90, 30.47, 30.26, 29.67, 29.55, 29.44, 29.40, 29.32, 22.67, 14.11. A satisfactory analysis was not obtained. Anal. Calcd for $C_{28}H_{58}S_2$: C, 73.29, H, 12.74. Found: C, 73.75, H, 12.59.

2-Octyl-2-pentadecylpropane-1,3-dithiol (5; C10C17(SH)$_2$). ^{1}H NMR (300 MHz, $CDCl_3$): δ 2.52 (d, J = 9.3 Hz, 4 H, SCH_2), 1.37−1.22 (m, 42 H), 1.08 (t, J = 9.3 Hz, 2 H, SH), 0.88 (t, J = 7.7 Hz, 6 H, CH_3). ^{13}C NMR (75 MHz, $CDCl_3$): δ 39.76, 33.60, 31.92, 30.44, 30.25, 29.67, 29.54, 29.46, 29.39, 29.30, 22.67, 14.12. Anal. Calcd for $C_{26}H_{54}S_2$: C, 72.48, H, 12.63. Found: C, 72.79, H, 12.45.

Preparation of SAMs. Solutions of the chelating alkanedithiols (ca. 1 mM) were prepared in weighing bottles that were pre-cleaned by soaking for 1 h in "piranha" solution (ca. 7/3 H_2SO_4/H_2O_2) (*caution: "piranha" solution reacts violently with organic materials and should be handled carefully*). The bottles were thoroughly rinsed with deionized water and absolute ethanol and dried before use. Silicon wafers, which were coated with ca. 2,000 Å of freshly evaporated gold,[27] were cut into slides (ca. 1 cm × 3 cm) using a diamond-tipped stylus. The slides were washed with absolute ethanol and dried under a flow of ultrapure nitrogen. The slides were immersed in solutions of the respective thiols in isooctane and allowed to equilibrate for 48 h. Before characterization, the resultant SAMs were thoroughly rinsed with both toluene and ethanol and blown dry with ultrapure nitrogen.

Ellipsometric Thickness Measurements. The thicknesses of the SAMs were measured using a Rudolf Research Auto EL III ellipsometer equipped with a He−Ne laser operating at a wavelength of 632.8 nm and an angle of incidence of 70°. Immediately after evaporating gold onto the chromium-primed Si wafers,[27] the optical constants for the

(19) Garg, N.; Lee, T. R. *Langmuir* **1998**, *14*, 3815.
(20) Xiao, X.; Hu, J.; Charych, D. H.; Salmeron, M. *Langmuir* **1996**, *12*, 235.
(21) McDermott, M. T.; Green, J.-B.; Porter, M. D. *Langmuir* **1997**, *13*, 2504.
(22) Lio, A.; Charych, D. H.; Salmeron, M. *J. Phys. Chem. B* **1997**, *101*, 3800.
(23) Lee, S.; Shon, Y.-S.; Colorado, R., Jr.; Guenard, R. L.; Lee, T. R.; Perry, S. S. *Langmuir* **2000**, *16*, 2220.
(24) Kim, H. I.; Koini, T.; Lee, T. R.; Perry, S. S. *Langmuir* **1997**, *13*, 7192.
(25) Perettie, D. J.; Morgan, T. A.; Zhao, Q.; Kang, H.-J.; Talke, F. E. *J. Magn. Magn. Mater.* **1999**, *193*, 318.
(26) Kondo, H.; Hisamichi, Y.; Kamei, T. *J. Magn. Magn. Mater*. **1996**, *155*, 332.
(27) Shon, Y.-S.; Lee, T. R. *Langmuir* **1999**, *15*, 1136.
(28) Shon, Y.-S.; Colorado, R., Jr.; Williams, C. T.; Bain, C. D.; Lee, T. R. *Langmuir* **2000**, *16*, 541.

bare gold were measured. To calculate the thicknesses of the SAMs, a refractive index of 1.45 was assumed for all films. The data were collected and averaged over at least three separate slides using three spots per slide for each type of SAM.

X-ray Photoelectron Spectroscopy (XPS). X-ray photoelectron spectra of freshly prepared samples were obtained using a PHI 5700 X-ray photoelectron spectrometer equipped with an monochromatic Al Kα X-ray source ($h\nu = 1486.7$ eV) incident at 90° relative to the axis of a hemispherical energy analyzer. The spectrometer was operated at high resolution with a pass energy of 23.5 eV, a photoelectron takeoff angle of 45° from the surface, and an analyzer spot diameter of 1.1 mm. Spectra were collected at room temperature and a base pressure of 2×10^{-9} Torr for C 1s, S 2p, and Au 4f. Standard curve-fitting software using Shirley background subtraction and Gaussian−Lorentzian profiles was used to determine the peak intensities. The peaks were fit with respect to spin−orbit splitting (two 65% Gaussian curves in a 3:4 area ratio split by 3.67 eV for Au 4f peaks).

Infrared Spectroscopy. Polarization modulation infrared reflection absorption spectroscopy (PM-IRRAS) data were obtained using a Nicolet MAGNA-IR 860 Fourier transform spectrometer equipped with a liquid nitrogen-cooled mercury−cadmium−telluride (MCT) detector and a Hinds Instruments PEM-90 photoelastic modulator operating at 37 kHz. The polarized light was reflected from the sample at an angle of incidence of 80°. The spectra were collected over 256 scans at a spectral resolution of 4 cm^{-1}.

Contact Angle Measurements. Advancing contact angles of various liquids were measured at 293 K and ambient relative humidity using a ramé-hart model 100 contact angle goniometer. The contacting liquids were dispensed and withdrawn at the slowest possible speed (ca. 1 μL/s) using a Matrix Technologies micro-Electrapette 25. The measurements were performed while keeping the pipet tip in contact with the drop. The data were collected and averaged over at least three separate slides using three spots per slide for each type of SAM.

Atomic Force Microscopy (AFM). For topographic and frictional studies, the Au(111) surfaces were prepared by annealing a gold wire in a flame of H_2/O_2 to produce a number of atomically flat (111) terraces around the circumference of the resultant gold microball. Detailed procedures for the preparation and characterization of these gold substrates have been described in a previous report.[24] The AFM instrument employed here utilized a conventional beam deflection technique with a single tube scanner (0.5 in. in diameter and 1.0 in. in length).[24] In this technique, light from a laser diode was focused on the backside of the V-shaped microfabricated cantilever, which supported the probe tip protruding from underneath. The sample was scanned relative to a fixed cantilever position. Deflections of the cantilever generated by interaction of the probe tip and the sample surface were detected by a four-quadrant position-sensitive detector. With this approach, both normal and lateral deflections of the cantilever were simultaneously recorded. For frictional characterization, normal forces reflect the load and lateral forces reflect the frictional response. The load data were calibrated using the normal force constant of the cantilever assembly provided by the manufacturer (Digital Instruments, 0.58 N/m). The frictional responses are reported as the amplified photodiode response (volts). Sample positioning as well as data collection and processing were controlled by RHK AFM 100 and RHK STM 1000 electronics and software.

Results

Ellipsometry of the SAMs. Figure 2 plots the measured ellipsometric thicknesses vs the adsorbates **1**−**6** used to generate the SAMs. These data highlight at least two important features regarding spiroalkanedithiol-based SAMs. First, the adsorbates generate monolayer rather than multilayer films. Second, by shortening one of the two alkyl tail groups of the unsymmetrical 2,2-dialkylpropane-1,3-dithiols, the effective film thicknesses can be controlled at the angstrom level. Indeed, the measured thicknesses systematically decrease across the series **1**−**5**, suggesting that the unsymmetrical SAMs derived from **2**−**5** possess molecular packing densities comparable to that of the symmetrical SAM derived from **1**. Given the structures of the adsorbates, we propose that SAMs derived from **2**−**5** are probably well packed near the surface but loosely packed near the terminal regions of the film.

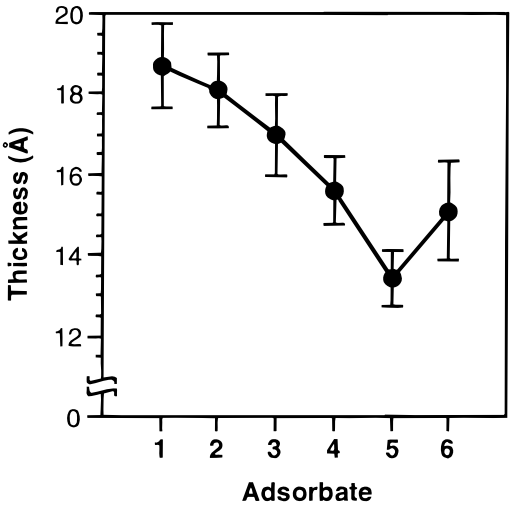

Figure 2. Ellipsometric thicknesses of the SAMs on gold derived from **1**−**6**. Average values of at least nine independent measurements are reported. The line through the data is provided solely as a guide to the eye.

Interestingly, the ellipsometric data show a greater effective thickness for the SAM derived from **6** than for the SAM derived from **5,** even though **6** contains only a single alkyl tail group per two sulfur head groups. While these results might appear anomalous, the data are consistent with XPS studies (vide infra) and suggest a distinct adsorption geometry of the dithiol species possessing only a single alkyl chain.

XPS of the SAMs. X-ray photoelectron spectroscopy (XPS) has been used to evaluate the relative atomic composition present on the surface of self-assembled monolayer films.[29,30] As demonstrated in previous reports,[23,28] comparison of the relative intensities of carbon and gold can provide information regarding the packing densities in these films. Indeed, since the observed intensities of Au are dependent on the amount of C overlayer adsorbed, these data can provide an indirect comparison of the density of carbon for each system. The data collected here (Figure 3) show that the integrated peak area of Au 4f increases linearly from **1** (169027 au) to **5** (215193 au). However, the XPS data for **6** (197615 au) appear anomalous, as observed with the thickness data (Figure 2). These results suggest that the carbon overlayer coverage is greater for SAMs derived from **6** than those derived from **5**.

The relative densities of alkyl chains in these films can be calculated using the method described in a previous report.[28] The present results indicate a 67% coverage of alkyl chains for SAMs derived from **6** relative to a 100% coverage for SAMs derived from **1**, which agrees well with previous studies by XPS of these two types of SAMs.[23,28] Correspondingly, the sulfur atoms in **6** are more densely packed on the surface than those derived from **1** (and presumably those derived from **2**−**5**). The low effective volume of **6** and the availability of multiple adsorption sites on gold apparently gives rise to the relatively high S/Au ratio for SAMs derived from **6**.[28]

PM-IRRAS of the SAMs. Figure 4 shows the C−H stretching region of the PM-IRRAS spectra obtained for the

(29) Bain, C. D.; Whitesides, G. M. *J. Phys. Chem.* **1989**, *93*, 1670.
(30) Hutt, D. A.; Leggett, G. J. *J. Chem. Phys.* **1996**, *100*, 6657.

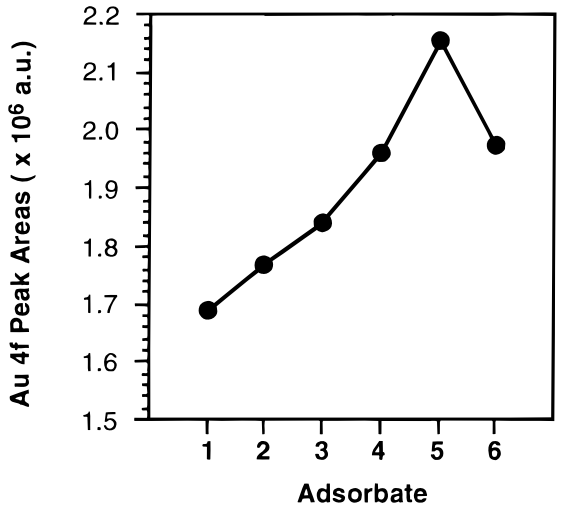

Figure 3. Integrated peak areas of Au 4f X-ray photoelectron spectra (XPS) of SAMs on gold derived from **1**−**6**. The uncertainty in the values of integrated peak area falls within the size of the symbol.

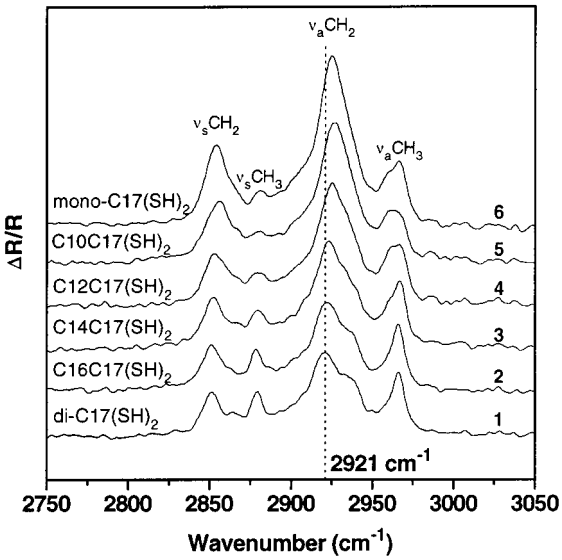

Figure 4. Surface infrared spectra (PM-IRRAS) of the SAMs on gold derived from **1**−**6**. The differential surface reflectivity ($\Delta R/R$) was calculated as the ratio $(R_p - R_s)/(R_p + R_s)$, where R_p and R_s represent the reflectivity for the respective polarizations of light.

SAMs derived from compounds **1**−**6**. In evaluating the data from the PM-IRRAS measurements, we focus our attention on the frequency of the methylene antisymmetric C−H stretch ($\upsilon_a^{CH_2}$), because this band is highly sensitive to the degree of order (or crystallinity) of the films; the lower the value of $\upsilon_a^{CH_2}$, the greater the crystallinity of the SAM.[8] As with the ellipsometry data shown in Figure 2, a plot of the $\upsilon_a^{CH_2}$ band position vs adsorbates **1**−**6** (Figure 5) shows a systematic trend across the series from **1** to **5**, and the data for **6** appear anomalous. For SAMs derived from **1**−**5**, the position of the $\upsilon_a^{CH_2}$ band shifts systematically from 2921 cm^{-1} (for **1**) to 2927 cm^{-1} (for **5**). The trend in the data thus indicates the alkyl chains of the SAMs derived from **1** are the most crystalline, and those derived from **5** are the most "liquid-like"; the degree of crystallinity of the SAMs derived from **2**−**4** falls uniformly between these two limiting values. The PM-IRRAS data are further consistent with a model for SAMs derived from **2**−**5** in which the adsorbate packing near the surface is comparable to that of **1**, but the alkyl chains become progressively more loosely packed near the terminal regions of the film during the stepwise progression

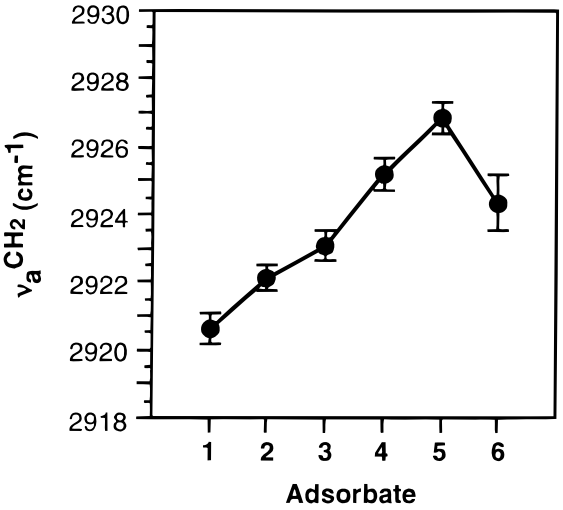

Figure 5. Antisymmetric methylene ($\upsilon_a^{CH_2}$) band position vs the adsorbate used to prepare SAMs on gold. The line through the data is provided solely as a guide to the eye.

Table 1. Advancing Contact Angles of Various Liquids on SAMs Derived from **1**−**6**[a]

adsorbate	H_2O	FA	DI	BN	DC	HD
1	114	98	72	68	52	48
2	113	97	71	67	50	46
3	112	96	70	65	46	41
4	109	93	67	62	34	27
5	105	89	62	53	30	<10
6	108	91	64	57	36	34

[a] H_2O = water; FA = formamide; DI = diiodomethane; BN = α-bromonaphthalene; DC = decalin; HD = hexadecane. Measured values were reproducible within ±2° of the reported values.

from **1** to **5**. This model assumes similar adsorption geometries for spiroalkanesdithiols **1**−**5** on the Au(111) surface (vide supra).

Given the molecular structures of **1**−**6**, SAMs generated from **6** appear to be more crystalline than expected with $\upsilon_a^{CH_2} = 2924$ cm^{-1}. As with the ellipsometric and XPS data discussed above, this apparent anomaly probably arises from the fact that the sulfur atoms in adsorbed **6** are packed more densely on the surface of gold than those in adsorbed **1**−**5** (vide supra).[28]

Wettabilities of the SAMs. The advancing contact angles (θ_a) measured for several liquids in contact with the surfaces of the SAMs derived from **1**−**6** are provided in Table 1 and presented graphically in Figure 6. We chose liquids ranging from polar protic (water and formamide) to polar aprotic (diiodomethane and α-bromonaphthalene) to apolar aprotic (decalin and hexadecane) to provide a comprehensive evaluation of the interfacial energies of the SAMs.[11,31,32] Due to the magnitude of their surface tensions, the latter two liquids are highly sensitive to small changes in the interfacial free energy of hydrocarbon surfaces. Moreover, due to intercalation processes, hexadecane is particularly sensitive to small changes in the interfacial structure of organic films composed of long alkyl chains.[7,11]

The trends in Figure 6 are consistent with the trends in the ellipsometric, XPS, and PM-IRRAS data: the advancing contact angles decrease progressively through the series from **1** to **5**, and then increase slightly for **6**. Since interfacial methylene

(31) Fowkes, F. M.; Riddle, F. L., Jr.; Pastore, W. E.; Weber, A A. *Colloids Surf.* **1990**, *43*, 367.
(32) van Oss, C. J.; Chaudhury, M. K.; Good, R. J. *Adv. Colloid Interface Sci.* **1987**, *28*, 35.

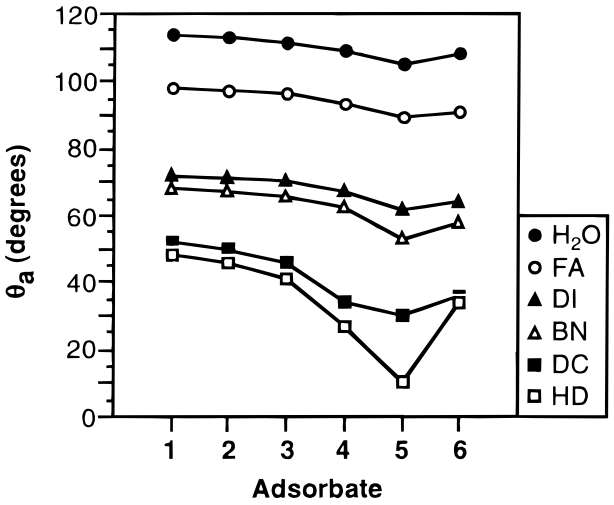

Figure 6. Advancing contact angle vs the adsorbate used to prepare SAMs on gold. The lines through the data serve only as guides to the eye. H_2O = water; FA = formamide; DI = diiodomethane; BN = α-bromonaphthalene; DC = decalin; HD = hexadecane. Measured values were reproducible within the size of the symbols.

Table 2. Receding Contact Angles of Various Liquids on SAMs Derived from **1**−**6**[a]

adsorbate	H_2O	FA	DI[b]	BN	DC	HD
1	103	87		57	41	37
2	102	87		55	38	35
3	101	86		53	34	28
4	98	83		50	21	13
5	93	76		40	17	<10
6	97	79		46	24	21

[a] H_2O = water; FA = formamide; DI = diiodomethane; BN = α-bromonaphthalene; DC = decalin; HD = hexadecane. Measured values were reproducible within ±2° of the reported values. [b] Receding contact angles of DI were not reproducible (always less than 30°) due to damage of the films by DI.[7]

groups are more wettable than interfacial methyl groups (vide infra),[7,11,33] the wettability data suggest that the fraction of accessible methylene moieties increases through the series from **1** to **5**, and then decreases slightly for **6**, where the fraction of accessible methylene groups appears comparable to that for **4**. The degree of exposure of methylene groups indicated by the wetttability measurements is consistent with the degree of crystalline order indicated by the PM-IRRAS measurements. That is, when taken together, the wettability and PM-IRRAS data show that liquidlike films possess a high fraction of accessible interfacial methylene moieties, a correlation entirely consistent with expectations.[7,11,33]

We also collected receding contact angles (θ_r) on these SAMs. Table 2 provides these data, which mirror the trends observed for the advancing contact angles. A plot of the contact angle hysteresis ($\Delta\theta = \theta_a - \theta_r$) is shown in Figure 7. Since the magnitude of $\Delta\theta$ can be used to evaluate the degree of heterogeneity of interfaces,[11,12] the consistently low values of $\Delta\theta$ shown here for all of the liquids on all of the SAMs argue strongly that the alkyl tail groups for SAMs derived from **1**−**6** are evenly distributed and/or homogeneously mixed across the surface.

Frictional Properties of the SAMs. Because the nonequivalent tail groups of SAMs derived from unsymmetrical spiroalkanedithiols are well-mixed at the molecular level,[18] the study of these SAMs provides an unprecedented opportunity to

(33) Chaudhury, M. K. *Mater. Sci. Eng.* **1996**, *R16*, 97.

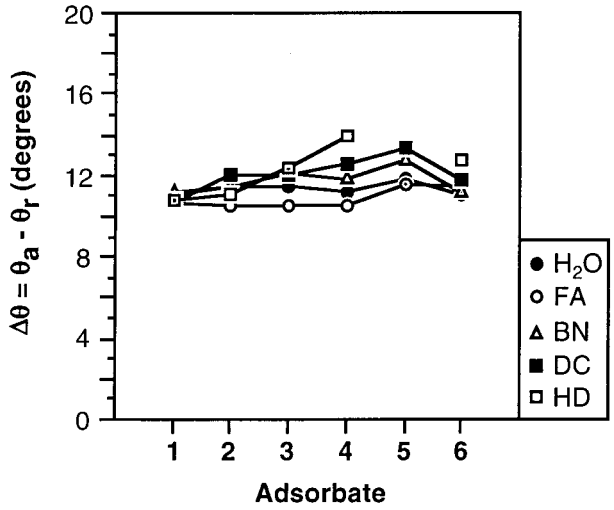

Figure 7. Contact angle hysteresis vs the adsorbate used to prepare SAMs on gold. The lines through the data serve only as guides to the eye. H_2O = water; FA = formamide; DI = diiodomethane; BN = α-bromonaphthalene; DC = decalin; HD = hexadecane. The uncertainty in the values of $\Delta\theta$ is within ±2° of the reported values. For SAMs derived from **5**, the value of θ_r^{HD} was less than 10°, which precludes the determination of a meaningful contact angle hysteresis for hexadecane on this SAM.

characterize the frictional properties of truly mixed organic monolayer films. In this work, by restricting the nonequivalency of the two alkyl chains to differences in their lengths, we can evaluate the frictional properties on the basis of structural parameters while excluding any differences arising from functional group (i.e., chemical) composition.

Before measuring the frictional responses of the SAMs derived from **1**−**6**, we examined their structural features by collecting topographic and lateral force AFM images over two different length scales: 1 μm × 1 μm and 50 Å × 50 Å. Over both length scales, the topographic images, which were collected simultaneously with the lateral force images, showed that the surfaces of all films were smooth and featureless except for the appearance of steps and terraces associated with the underlying gold substrates (rms roughness ≤ 3 Å/1 μm^2). Correspondingly, the lateral force measurements showed homogeneously distributed frictional properties. While these data and those collected above are consistent with a model in which the tail groups of the SAMs derived from **1**−**6** are evenly distributed and/or homogeneously mixed,[18] topographic imaging at small length scales (≤5 nm × 5 nm) failed to resolve molecular-level structures or packing orientations for these films.

We examined the frictional properties of the SAMs derived from **1**−**6** by measuring frictional forces as a function of load over several different areas of the film surfaces.[24] Figure 8a provides representative friction-load plots obtained for each type of SAM for decreasing applied loads (i.e., the unloading regime). Conventionally, these plots express attractive forces between the AFM tip and the film surfaces as negative loads. For a direct comparison of the frictional properties of the films, we used the same tip-cantilever assembly for all of the measurements. In addition, to avoid any potential artifacts associated with using the same tip-cantilever on consecutive samples, we randomly altered the sequence of data acquisition. Figure 8b provides a quantitative comparison of the frictional properties of the films by plotting the frictional response obtained at 20 nN in both the loading and the unloading regimes; the error bars reflect the standard deviation from the average of five runs across each

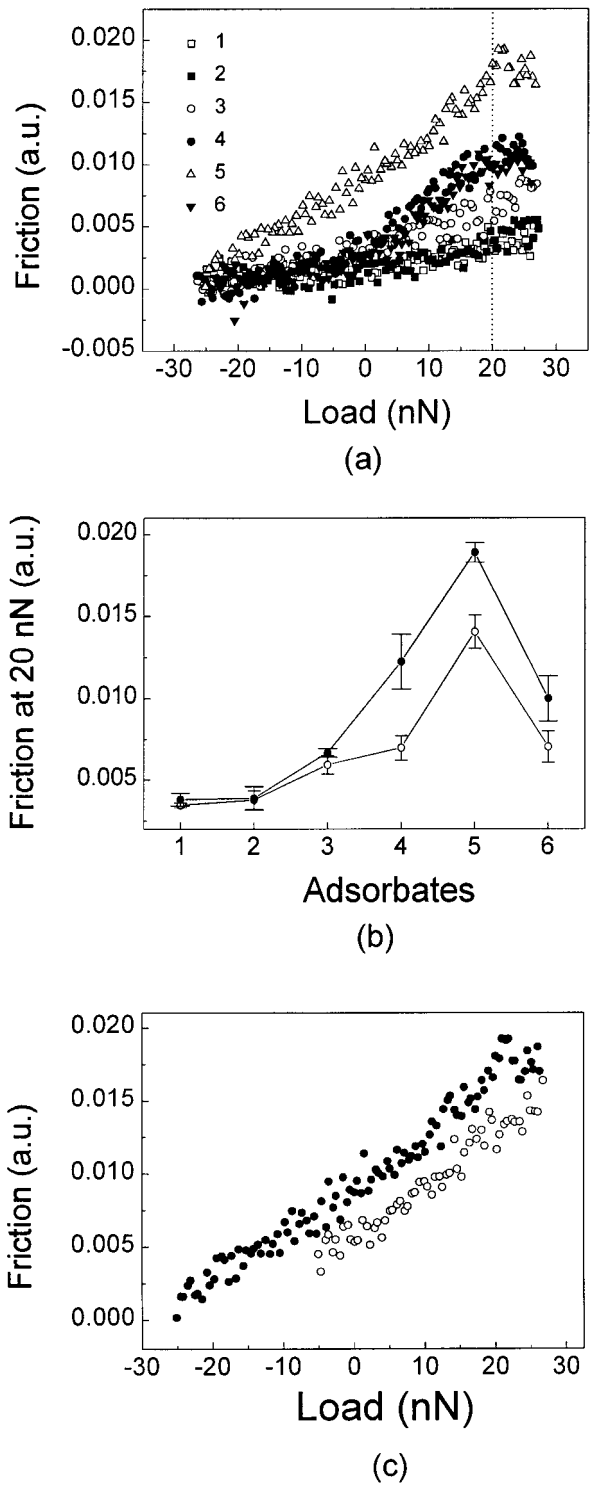

Figure 8. (a) Friction-load plots for the SAMs derived from **1**−**6**. The trends in the data and the values of the pull-off forces in the negative load regime were reproducible over five independent measurements for each adsorbate. (b) Frictional response obtained at 20 nN in both loading and unloading regimes for the SAMs derived from **1**−**6**. (c) Frictional hysteresis loop obtained on the SAM derived from **5**. In both (b) and (c), the symbol ○ represents data collected during loading, while the symbol ● represents data collected during unloading.

sample. Taken together, plots a and b in Figure 8 can be used to characterize the frictional properties of the films.[23,24]

First, we note that the frictional responses of the films vary systematically with their ellipsometric thicknesses, crystallinities, and wettabilities. Indeed, the trends in the data illustrated in Figure 8b show that the frictional properties of the SAMs increase through the series from **1** to **5**, and then decrease slightly for **6**. Previous studies by AFM of the frictional properties of hydrocarbon self-assembled films have highlighted the correlation between the frictional response and the crystalline packing of the alkyl chains in SAMs: conformationally disordered hydrocarbon films exhibit higher frictional responses than highly crystalline hydrocarbon films.[18,20,22,23] Given the systematic variation of the chain lengths of the spiroalkanedithiols **1**−**5**, it is reasonable to assume that the local structure of the alkyl chains near the terminal portion of the SAMs is different from that near the sulfur atoms. Through the series from **1** to **5**, the gradual decrease of the *average* packing density and/or crystallinity of the alkyl chains arises from the progressive increase of the loosely packed fraction near the top and the corresponding decrease of the more densely packed fraction near the bottom of the films. Among these highly correlated structure/property relationships, it is interesting to note that the wettability and frictional responses of SAMs derived from **4** and **6** are similar despite the obviously different structural arrangement of the alkyl chains in these two SAMs. The data presented here therefore suggest that the primary factor influencing these interfacial properties (i.e., wettability and friction) arises from the *average* packing density and/or crystallinity of the alkyl chains rather than their specific structural arrangement.

Second, despite the systematic variation in the frictional responses, the adhesive forces between the tip and the samples as measured from the pull-off forces during sliding are indistinguishable for all films (i.e., as shown in Figure 8a, the value of the negative load during snap-off is the same for all films). Moreover, indistinguishable pull-off forces for all films were reproducibly obtained even when the lateral displacement between the tip and the samples was disabled (data not shown). While these results might appear surprising in light of the observed trends in the contact angle data (which correlate directly with the interfacial works of adhesion),[32] the JKR theory of adhesion mechanics predicts similar pull-off forces for these chemically similar films.[33−35] As in related systems,[23,24] we note that SAMs derived from **1**−**6** give rise to predominantly van der Waals forces across their interfaces. In contrast, SAMs exposing polar and/or acid−base moieties exhibit enhanced pull-off forces when contacted with either bare silicon nitride or chemically functionalized AFM tips.[36−38]

Third, comparison of the frictional responses obtained during loading vs unloading shows an enhanced frictional hysteresis for the least crystalline films. Examination of Figure 8b reveals no detectable frictional hysteresis for the SAMs derived from **1** and **2**, but significant frictional hysteresis for the other SAMs, particularly those derived from **4**−**6**. For the latter SAMs, the frictional responses collected in the loading regime were always lower than those collected in the unloading regime. For the purpose of illustration, Figure 8c shows the hysteresis loop obtained for the SAM derived from **5**, which exhibits both the least crystallinity and the maximum frictional hysteresis. The hysteresis shown in Figure 8c is, in fact, similar to that previously reported for other "liquid-like" SAMs, such as those generated from C-6 normal alkanethiols and alkylsilanes.[22]

(34) Johnson, K. L.; Kendall, K.; Roberts, A. D. *Proc. R. Soc. London* **1971**, *A324*, 301.
(35) Israelachvilli, J. *Intermolecular and Surface Forces*; Academic: London, 1992; pp 326−329.
(36) Frisbie, C. D.; Rozanyai, F.; Noy, A.; Wrighton, M. S.; Lieber, C. M. *Nature* **1994**, *265*, 2072.
(37) Sinniah, S. K.; Steel, A. B.; Miller, C. J.; Reutt-Robey, J. E. *J. Am. Chem. Soc.* **1996**, *118*, 8925.
(38) Ito, T.; Namba, M.; Buhlmann, P.; Umezawa, Y. *Langmuir* **1997**, *13*, 4323.

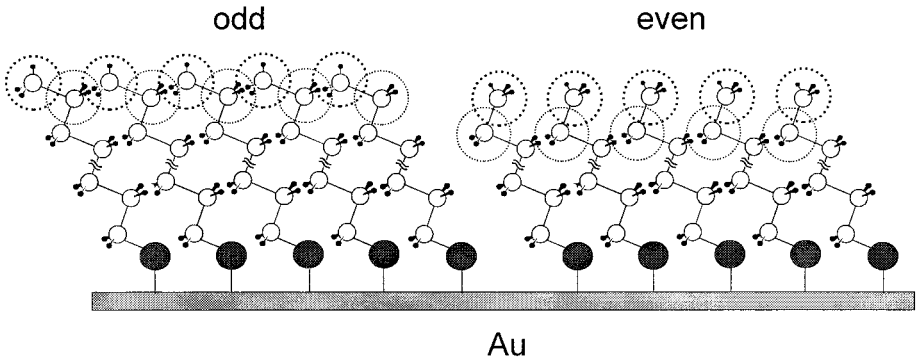

Figure 9. Illustration of the differing terminal group orientation that arises from normal alkanethiol-based SAMs composed of odd (left) vs even (right) chain lengths. SAMs composed of odd chain lengths expose a higher density of atomic contacts at the interface.

The correlation between the magnitude of the hysteresis and the degree of crystallinity of the alkyl chains can be rationalized as follows. For well-packed highly crystalline films (e.g., those derived from **1** and **2**), deformation of the film by the AFM tip during the loading process (maximum $\leq$30 nN) appears to be instantaneously and elastically recovered during the unloading process, giving rise to indistinguishable frictional responses in the loading and unloading regimes. In contrast, however, loosely packed liquid-like films (e.g., those derived from **4**−**6**) appear to undergo a quasiplastic deformation upon contact with the AFM tip during the loading process. This quasiplastic deformation appears to be sufficiently long-lived to give rise to the enhanced frictional response observed during the unloading process. We note that imaging of the line scanned in the friction-load measurements failed to reveal changes in either the topographic or lateral force images (200 nm $\times$ 200 nm) of a freshly prepared film. Upon scanning a single line $\sim$100 nm in length at loads sufficiently high to remove the SAM from the surface of gold (e.g., $\geq$200 nN), however, the scanned line could be readily imaged over scan areas of 200 nm $\times$ 200 nm.[39] Apparently, the degree of deformation at maximum loads of $\leq$30 nN is insufficient to effect changes in the topographic and lateral force images, but sufficient to effect changes in the frictional hysteresis.

Discussion

The results presented above demonstrate that the crystallinity, wettability, and tribological properties of SAMs on gold can be specifically tailored by systematically varying the length of one alkyl chain in spiroalkanedithiol-based adsorbates. The wide range of interfacial wettabilities and frictional responses reported here are particularly surprising given that the tail groups of the SAMs are purely hydrocarbon in nature. Furthermore, the precise control over the interfacial structure afforded by spiroalkanedithiol-based SAMs permits new insight into the origins of interfacial friction and wettability in organic thin films.

The data obtained here clearly demonstrate a high degree of correlation between the crystalline order of hydrocarbon-based SAMs and their frictional properties. Two distinct but mutually compatible hypotheses have been advanced to rationalize this type of correlation. The first hypothesis argues that conformational defects in SAMs having loosely packed alkyl chains give rise to additional channels of energy dissipation and thus enhanced frictional responses during sliding.[20,22] The second hypothesis argues that loosely packed alkyl chains undergo enhanced van der Waals contact with the AFM tip, which gives rise to enhanced frictional responses during sliding.[18,23] In the latter model, we proposed that the number of atomic contacts falling within a given area of contact is greater for liquid-like films than for crystalline films. We based our reasoning on the fact that the length of a C−C bond (1.54 Å) is substantially shorter than the intermolecular distance between terminal methyl groups in well-packed, well-ordered SAMs on gold (4.99 Å). Consequently, we argued that the van der Waals interactions between an AFM tip and the terminal hydrocarbon backbones of liquid-like SAMs are greater per unit area than those between an AFM tip and the terminal methyl groups of crystalline SAMs. These additional van der Waals interactions can plausibly enhance the static and kinetic frictional responses by increasing the shear force per unit area of contact.[23] We believe that the frictional data reported here (Figure 8) are entirely consistent with this model. We note, however, that an increase in the number of atomic contacts per unit area is perhaps unlikely to be the sole contributor to the approximately 7-fold variation in frictional response observed across the series in Figure 8. Thus, while we believe that the van der Waals model represents a substantial channel of energy dissipation that must be considered when evaluating the molecular origins of friction in organic thin films, we believe that other phenomena, such as conformational defects[20,22] and/or dislocation mechanisms,[33,40] should also be considered.

Of further relevance to our frictional studies is a recent report by Porter and co-workers, which found that the frictional properties of hydrocarbon-terminated SAMs having odd-numbered chain lengths were higher than those of analogous SAMs having even-numbered chain lengths.[41] In their analysis, the authors argued that the systematic difference in frictional response arose from dipole-based differences in the surface free energy of SAMs having odd vs even chain lengths. We believe that our model of frictional response based on van der Waals interactions between the films and the contacting AFM tip (presented above and elsewhere)[18,23] can also be used to rationalize the parity effect observed by Porter and co-workers.

Consider, for example, the orientation of the terminal CH_2-CH_3 bonds in normal alkanethiol-based SAMs on gold (Figure 9). At the film terminus, the "odd" SAMs expose a mixture of CH_2 and CH_3 groups, while those of "even" SAMs expose only CH_3 groups. Consequently, at low contacting loads such as those employed here, the density of atomic contacts between an "odd" film and an AFM tip will be greater than that between an "even" film and an AFM tip (assuming that the overall area of contact is constant from sample to sample). This difference in the number of atomic contacts per unit area

(39) Liu, G.-Y.; Salmeron, M. *Langmuir* **1994**, *10*, 367.

(40) Ghatak, A.; Vorvolakos, K.; She, H.; Malotky, D. L.; Chaudhury, M. K. *J. Phys. Chem. B* **2000**, *104*, 4018.

(41) Wong, S. S.; Takano, H.; Porter, M. D. *Anal. Chem.* **1998**, *70*, 5209.

would predict stronger van der Waals interactions between an "odd" film and an AFM tip compared to those between an "even" film and an AFM tip. The van der Waals model would thus predict a higher frictional response for "odd" films than for "even" films, which agrees with the experimental observations.[41]

We further propose that our model can be used to rationalize the previously observed "odd−even" wettability effects observed for normal alkanethiol-based SAMs on gold. For example, when using hexadecane as the contacting liquid, studies have consistently found that "odd" hydrocarbon SAMs are more wettable than "even" hydrocarbon SAMs.[42−45] By analogy to the differing interactions between an AFM tip and the surfaces of "odd" vs "even" SAMs, we propose that the contacting hexadecane molecules experience more atomic contacts per unit area on the surfaces of "odd" SAMs than on "even" SAMs. The corresponding enhanced van der Waals interactions between the contacting liquid and the "odd" SAMs thus give rise to the enhanced wettability of the "odd" SAMs.

The van der Waals-based model of wettability described here might be used further to rationalize the commonly reported observation that surface methylene groups are more wettable than surface methyl groups.[7,11,33] In accord with the analysis presented above, surfaces composed of methylene groups necessarily expose a higher interfacial atomic density (and thus a greater van der Waals potential) than surfaces composed of methyl groups. We propose that it is precisely this difference in interfacial atomic density that gives rise to the enhanced wettability of surfaces composed of methylene groups.[46]

From a simplified perspective, our proposed rationalization for the observed trends in wettability is analogous to that used to rationalize the observed trends in the boiling points of linear vs branched isomeric hydrocarbons. Consider, for example, that the boiling point of linear *n*-octane is 125.7 °C, and that for the branched isomer, 2,2,3,3-tetramethylbutane, is 106.5 °C.[47] Because the degree of branching in the latter isomer reduces the intermolecular area of contact, the cohesive van der Waals forces in the former are greater than those in the latter.[48] We readily admit that the simple model of wettability presented here fails to consider the important contributions arising from the interfacial solid−vapor free energies (γ_{sv}) and the interfacial liquid−vapor free energies (γ_{lv}), which are related to the solid−liquid free energies (γ_{sl}) and the contact angles (θ) through Young's equation ($\gamma_{lv} \cos \theta = \gamma_{sv} - \gamma_{sl}$).[49] Moreover, we have entirely neglected the role of entropy.[7,11] Future studies will seek to provide a more quantitative analysis of the present data.

Conclusions

A series of specifically designed spiroalkanedithiols were used to prepare SAMs on gold in which the packing density and crystalline order of the hydrocarbon tail group assemblies were systematically varied. These structural variations strongly influenced both the interfacial wettabilities and the frictional properties of the SAMs. Measurements of advancing and receding contact angles for a variety of liquids on these SAMs showed that well-packed, highly crystalline tail group assemblies were less wettable than loosely packed, liquid-like tail group assemblies, presumably because the latter species expose a high fraction of methylene vs methyl moieties at the interface. Studies of the contact angle hysteresis were consistent with a model in which the hydrocarbon tail groups were evenly distributed and/or homogeneously mixed across the surface. Measurements of the frictional properties of the films by AFM were also found to correlate with the crystalline order of the films: liquid-like films exhibited higher frictional responses than conformationally ordered films. While systematic differences in the frictional properties of the SAMs were readily detected, no differences in the adhesive forces between the silicon nitride AFM tips and the SAMs could be detected. The liquid-like films also exhibited frictional hysteresis in which the frictional responses were lower in the loading regime compared to those in the unloading regime, perhaps due to a quasiplastic deformation of the SAMs by the AFM tip. The observed trends in wettability and friction appear to strongly correlate with the magnitude of the van der Waals interactions between the hydrocarbon tail groups and the contacting probe liquid and the AFM tip, respectively.

Acknowledgment. This research was generously supported by the National Science Foundation (DMR-9700662 and CAREER Award to T.R.L.: CHE-9625003) and the Robert A. Welch Foundation (Grant No. E-1320). This work made use of MRSEC shaved experimental facilities supported by the NSF (DMR-9632667). We thank Professor Manoj Chaudhury (Lehigh University) for many insightful discussions.

JA000403Z

(42) Miller, W. J.; Abbott, N. L. *Langmuir* **1997**, *13*, 7106.
(43) Garg, N.; Lee, T. R. *Langmuir* **1998**, *14*, 3815.
(44) Shon, Y.-S.; Lee, T. R. *Langmuir* **1999**, *15*, 1136.
(45) Graupe, M.; Takenaga, M.; Koini, T.; Colorado, R., Jr.; Lee, T. R. *J. Am. Chem. Soc.* **1999**, *121*, 3222.
(46) The rationalization presented here represents a slight variation in perspective from that offered by Bain et al. in refs 7 (p 326) and 11 (p 7173).
(47) In *CRC Handbook of Chemistry and Physics*, 71st ed.; Lide, D. R., Ed.; CRC Press: Boca Raton, FL, 1990.
(48) Streitwieser, A., Jr.; Heathcock, C. H. In *Introduction to Organic Chemistry*, 2nd ed.; Macmillan: New York, 1981; pp 69−78.
(49) Young, T. *Philos. Trans. R. Soc.* (*London*) **1805**, *95*, 65.